Photocatalytic Studies on Zinc Oxide Nanoparticles Doped with Selenium and Silicon Dioxides for Photodegradation of Lasix Drug

L.Ramapriya[1]* and J.Santhanalakshmi[2]
[1]Department of Chemistry, Dr.M.G.R. Educational and Research Institute, Chennai
[2]University of Madras, Guindy Campus, Chennai, Tamilnadu, India.
*Email: toramapriya@gmail.com
Received: 20.7.2023, Revised: 2.11.2023, Accepted: 18.11.23

ABSTRACT

Metal oxide nanoparticles have taken a broad area of intense research because of their unique properties and application in diversified fields. Zinc oxide (ZnO) nanoparticles show varied morphologies and significant activities especially after doped with different metals. In this work, ZnO nanoparticles, Selenium dioxide (SeO_2) doped Zinc oxide nanoparticles and Silicon dioxide (SiO_2) doped Zinc oxide nanoparticles are synthesised by sol-gel method. The dopant effect on ZnO for band gap energy, crystal size and morphology are investigated by analysing the UV-DRS, powder X-ray diffraction and FESEM measurements respectively. The photocatalytic activities of these synthesised nanoparticles are compared by subjecting them into degradation of drug Lasix (furosemide) under UV and Solar irradiation sources. The progress of drug degradation is studied by measuring absorbance versus time interval at constant wavelength (325 nm) of the drug. The rate coefficient values found in this oxidative (H_2O_2) and reductive ($NaBH_4$) catalytic degradation process of the drug is found efficient in solar irradiations. The results of characterisation studies and the order of photocatalytic activities of the nanoparticles are discussed.

Keywords: ZnO nanoparticles, selenium dioxide doped ZnO nanoparticles, silicon dioxide doped ZnO nanoparticles, drug degradation

Introduction

In recent years, use of drugs to fight against infections and chronic illness has become unavoidable. The emergence of many chemically compounded drugs in medicine field has also increased more discharge in the environments. Especially, the water resources are contaminated with the discharge of popularly used drugs and those from the pharmaceutical manufacturing units[1]. Degradation followed by mineralisation of the water soluble drugs in trace amounts is mostly a slow process in nature. Heterogenous photocatalysis using nano crystalline semiconductors has emerged as a potential and developing advanced oxidation processes used in the remediation of industrial polluted water

DOI: 10.59143/isas.jisas.2.3.YHOJ2087

effluents[2]. Many transition metal oxides are used as catalysts for these processes[3,4]. In the present work, the use of photoactive metal oxides nanomaterials such as ZnO has been chosen to catalyse photo assisted degradation of Lasix a diuretic class of drug composed of furosemide.

The oxides of the p block elements were opted to dope so that the doping will activate the hole-pair movements during photo catalysis of ZnO[5-9]. ZnO doped with selenium also have photoelectronic properties and contribute to the crystallite size[10-11]. ZnO with dopants from p-block elements Selenium and Silicon were synthesised as nanoparticles and their photocatalytic activities were compared on degradation of furosemide drug. Regarding the irradiation sources, solar and UV are chosen for the study. Aqueous solutions of the drugs were used for the degradation in the oxidative degradation H_2O_2 was used while in reductive degradation $NaBH_4$ was used. The kinetics of degradation of the drug under the oxidation and reduction stresses was studied and the rate coefficient values were determined. Based on the kinetic parameters, the trend set in the degradation processes was evaluated. A plausible reaction pathway was formulated.

Experimental

Materials: Zinc acetate and Ethylene Glycol were purchased from Merck. Selenium dioxide and Silicon dioxide were purchased from SRL and Ethanol from Haymann. Lasix (Furosemide) was purchased from retail pharmacy store and used. Double distilled water was used all through the experiments. UV–Vis spectrometer; double beam, Techcom instrument with 1 cm path length quartz cuvettes was used. Bruker D8 advance diffractometer was used for XRD data. FESEM of the nanoparticles were measured using SU6600, HITACHI model operating at an accelerating voltage of 100 kV. Fourier transform infrared spectrometer (FT-IR Perkin-Elmer Spectrum 2000 Spectrophotometer) was used for the structural analysis. Shimadzu GCMS-QP2010 Ultra and Column: Restek; Rxi-5Sil-MS; 30 m – 25 mm ID was used for gas chromatography and mass spectra analysis in this research work.

Synthesis of Nanoparticles: Nanoparticles were synthesised by sol-gel method[12-14]. The nanocrystalline ZnO was prepared by dissolving the precursor zinc acetate powder in water. To this precursor solution, ethylene glycol (10% v/v of solution) was added in drops under stirring as a stabiliser and the stirring was continued for 1 h at 80 ^{0}C. The reaction mixture is cooled, centrifuged and the centrifugate is dried initially at about 80 ^{0}C and then annealed at 600-650 ^{0}C for 3 hrs.

The doped ZnO nanoparticles were prepared as 10% stoichiometric ratios of dopants precursors and Zinc acetate dissolved in solvents water and ethanol accordingly. The precursors were Selenium dioxide and Zinc acetate for Selenium doped ZnO; Silicon dioxide and Zinc acetate for Silicon dioxide doped Zinc oxide nanoparticles. The two corresponding precursor solutions were mixed under constant stirring and synthesis was continued as for undoped ZnO synthesis.

Photocatalytic studies: 0.5 mM Lasix solution was prepared using water. 1 mg / 20 mL of catalyst to Lasix solution was used for all photocatalytic studies. For oxidative conditions H_2O_2 (30%) 1.0 mL and in reductive conditions, $NaBH_4$ (10%) 10 ml were used. All the solutions were prepared freshly and used. One pot batch type reactor with the nanomaterial and the substrate solution was set up. For this mixture with and without the addition of Hydrogen peroxide / Sodium borohydride, the absorbance maxima with respect to wavelength were recorded and this wavelength maxima (325 nm) was kept constant while the absorbance change during irradiation was recorded at definite intervals of time. The reaction mixture was irradiated with UV emitting lamps for UV irradiations (~250 nm). For solar irradiation, the reaction mixture was exposed to direct visible light. Absorbance variation plots were made. The kinetic plots for the rate constant determination were drawn from log (OD_0/OD_t) versus time data. The pseudo-first order rate coefficient values were determined by multiplying 2.303 with the slopes of the linear kinetic plots.

GC MS analysis: The kinetics of degradation of Lasix was monitored by measuring the change in absorbance values respective to the drug. Though the change in absorbance values directly reflects the change in concentration of the substrate, the degradation of compound and the formation of fragments were confirmed through GC instrument equipped with Mass analyser[15,16]. The column oven temperature was 40 ^{0}C and the sample was injected at 280 ^{0}C. The analysis was done with following specifications; Pressure :49.7 kPa, Total Flow :54.1 mL/min and Column Flow: 1.00 mL/min with Linear Velocity :36.1 cm/sec and Purge Flow :3.0 mL/min. The fragments separated through column were subjected to mass analyser where the fragments produced by ionization sources (280 ^{0}C) were detected with detectors running at 0.87 kV from 50 m/z to 450 m/z.

Results and Discussion:

UV- DRS measurements: In Fig 1, UV-DRS spectra of pure ZnO nanoparticles and doped ZnO nanoparticles with variation in the dopant's nature are given. By applying the tauc

relation $\alpha h\nu = a(h\nu - E_g)^n$, where 'a' is absorption coefficient and E_g the optical band gap, the band gap energy values of nanopowders of ZnO are determined for direct band gap energy value, n=2 has been used. For dopants, it may be seen that band gap energy values have increased to 3.27 eV and 3.3 eV respectively for SeO_2 and SiO_2 from 3.20 eV of undoped ZnO nanoparticles (Table 1). Hence, it is clearly evident that the band gap energy values of ZnO nanopowders are tunable for increased band gap energy values by dopants[17-20]. This effect can be utilised for shifting in the photocatalytic activity and photo absorption activity of ZnO nanoparticles both in solar and UV regions.

Size measurements: In Fig. 2, the powder x-ray diffractograms are presented for the undoped ZnO nanoparticles and doped ZnO nanoparticles are given. For undoped, the characteristic peaks appeared at angles (2θ) of 31.767, 34.420, 36.252, 47.537, 56.593, 62.853, 66.373, 67.944 and 69.083 corresponding to planes (0 1 0), (0 0 2), (0 1 1), (0 1 2), (1 1 0), (0 1 3), (0 2 0), (1 1 2) and (0 2 1) of hexagonal wurtzite phase; Zincite structure, space group p63mc and matches with ICSD card 76641. The lattice parameters are found to be a = b = 3.25 nm, c = 5.20 nm and $\alpha = \beta = 90^0$, $\gamma = 120^0$ respectively. For both the doped nanoparticles; similar pattern is observed, no impurity phase is found, except for change in crystallite size which was calculated from Scherrer equation ($\lambda = 1.54\ A^0$). The variation in the nano sizes of crystal sizes are found to decrease in case of dopants (Table 1). The inclusion of dopants in the crystal should have caused broad peak during diffraction (lattice disorder) resulting in decrease in the crystallite sizes[21-23]. Although the crystal sizes are calculated from PXRD measurements using Scherrer equation, these inferences are visible in the FESEM photographs (Fig.3). For silicon doping bullet type elongated particles are observed to be formed. In case of selenium too, the hybrid alterations of silicon and tellurium are seen. Based on the size measurements adopted using PXRD and FESEM, the trend observed in the nano size variations among pure ZnO nanocrystals and doped ZnO crystals is as follows:

Pure ZnO nanoparticles > SeO_2 doped ZnO nanoparticles > SiO_2 doped ZnO nanoparticles

FTIR measurements: Using K-Br pellets, the FTIR spectra of pure and doped ZnO nanoparticles recorded within the range of 4000-400cm^{-1} are shown in Fig 4. Regarding metal oxide nanoparticles in the pure form and as well as in the doped form, FTIR spectroscopy plays a significant role in characteristic peaks of metal oxides[24,25]. A doublet like strong peaks at 445 and 488cm^{-1} in the Fig 4 reveals that pure ZnO characteristic peak are being

present and in many literature reports, such peaks have been reported in the as synthesized condition. Upon doping, it is found that in most cases, the peaks are blue shifted and in some cases red shifted. In general, vibration bands around 445cm^{-1} to 530cm^{-1} could be assigned to Zn-O bond in the lattice. Adsorbed moisture and CO_2 in certain case may cause shifts. However, they are also reflected in the region 3200-3500cm^{-1} for weak O-H stretching bands. In case of SeO_2, a doublet around 497cm^{-1} and 447cm^{-1} are observed similar to undoped ZnO nanoparticles while 1030cm^{-1} may be attributed to Se-O bond. Additionally, a broad peak at 3418cm^{-1} seen is characteristic peak of adsorbed moisture, O-H bond. Selenium imparts partial or improved hygroscopicity to ZnO lattice. Regarding Silicon dopant, the characteristic peak of ZnO is broad and a triplet each at 532, 492 and 430 cm^{-1} are detected. Among these peaks 532 cm^{-1} addition to doublet of undoped ZnO, may be due to Si-O-Zn bond vibration. Si-O-Si characteristic peak is observed at 1110cm^{-1} in the ZnO lattice. The secondary vibration of Zn-O is mostly detected around 660-670cm^{-1} range. The peaks lying from 1500cm^{-1} to 1700cm^{-1} and 3200-3400cm^{-1} represents the C-O, O-H and C-H stretching due to adsorbed surficial CO_2 and H_2O molecules. Sometimes, these peaks also suffer strong shifts due to dopants lying at the surface.

Photocatalytic degradation studies: In Fig.5 typical UV-VIS spectrum of Lasix drug in concentration of 0.5 mM was given. Under the irradiation source, the variation in absorbance values with time was measured. In the absence of catalyst, mere oxidation of H_2O_2 to the drug solution caused the degradation appreciably only after 8h of the reaction. The degradation commenced instantly upon addition catalyst. During the start of the reaction, the mixture containing drug, with oxidant / reductant and the catalyst with irradiation show sharp changes in spectra. However, the changed spectra are retained until the completion of reaction. In Fig.6, the UV-Vis spectra of Lasix during the oxidative degradation by pure ZnO nanoparticles under solar irradiations stacked with respect to time has been shown and tabulated in table 2. The changes in the absorbance values at fixed λ_{max} of 325nm are taken and the absorbance versus time plots are prepared. The change in the absorbance values with respect to time are noted and used for the kinetic results.

Rate Coefficient Measurements: In Fig.7, the decrease in the absorbance values with time of progress of reaction is plotted under the oxidation stress for Lasix. All the three

synthesised nano catalysts have been used. The absorbance versus time plot for the solar assisted oxidative degradation of drug by the catalyst (Fig.7) shows there is a gradual decrease in the absorbance value. Since, pseudo first order reaction conditions were maintained, the first order plots for the rate coefficient values are given in the figure 8. The linear plots have confirmed the reaction followed via pseudo first order conditions and the slopes of the linear plots for the rate constant determination.

Replacing the solar irradiations by UV irradiations, the kinetic plots are made adopting similar measurement. The absorbance versus time plot and kinetic plot are given for the UV irradiation assisted oxidative reactions in Fig. 9 and 10 respectively. In table 3, the overall pseudo 1^{st} order rate constant values for both types of irradiations assisted oxidative degradation of the drug Lasix utilising undoped and various doped ZnO nano catalyst are given. Based on the rate constant values, the following trend set in the activity of the oxidative degradation of drugs can be envisaged. It is found that solar irradiations assisted degradation are faster than UV irradiations $K_{Solar} > K_{UVA}$. The values indicate that the degradation in solar is nearly three times faster than that in UV irradiations. The higher rate constant values obtained in the degradation by the doped nanoparticles from table 3, infer that the doped nanoparticles have higher photocatalytic activity than the undoped pure ZnO nanoparticles in degrading furosemide. Among the doped nanoparticles, SiO_2 doped ZnO nanoparticles possess higher rate coefficient values and the trend in photocatalytic activity follows the order of SiO_2 doped > SeO_2 doped > undoped ZnO nanoparticles.

However in the case of reduction using $NaBH_4$, the trend observed is undoped ZnO have higher photocatalytic rate coefficient values than that of dopants and the order is reversed (table 4). The altered trend between the oxidation and reduction stresses on Lasix may be due to the activity of p-block elements towards the peroxide radicals. In the case of reduction reactions, the nascent hydrogen utilised from $NaBH_4$ is quickly adsorbed on to the ZnO nanoparticles than the doped surfaces. Therefore, such a remarkable change in the dopant effect under the different redox stresses in the catalysis has been observed. It has been well proved in the literature intrinsic dopants have significantly altered the photocatalytic properties of metal oxide nanoparticles[26, 27].

Reaction Pathway: Furosemide is a potential diuretic pharmaceutical and susceptible to acid attacks due to secondary amine group presence. In order to rationalise the reaction pathway of the degradation of furosemide drug, the one pot bulk degradation of furosemide in

presence of ZnO catalyst for both oxidation and reduction reaction were performed separately. After the completion of the reaction for 2 hours, the catalyst removed product solutions were subjected to column chromatographic separation of degradation product. The major two separated products were analysed by GC-MS. Here also, during the scaling up of the reaction, photo irradiations were adopted. Both solar and UV irradiations were performed. It was found that the final products were nearly identical. In the oxidation mode, the hydrolysed product by H_2O_2 confirmed with CSA (4-chloro, 5- sulphamyl anthranilic acid) structure. The GC-MS of the products are given in Fig. 11. Also, the product solutions do not show any traces of unreacted furosemide. In the case of reduction reactions, the GC-MS of the major product supported the evidence of FSA (Furfuryl Sulphamoyl anthranilic acid). Minor quantities of furfuryl alcohol, levulinic acid and anthranilic acid altogether < 2% were detected. In the oxidation mode, methyl group attached to furan group was bifurcated while in reduction mode, dechlorination occurs[28-31]. The catalysis by ZnO nanoparticles is brought about in the enhanced production of electron hole pair during irradiation which in presence of H_2O_2 produced hydroxyl radicals and hydroperoxy radicals in sufficient extents. In the case of reduction mode, dechlorination is a possible route of degradation due to $H^{\bullet}$ radicals readily forming HCl. The dehydrochlorination product is most prevalent. The plausible schematic routes are presented below.

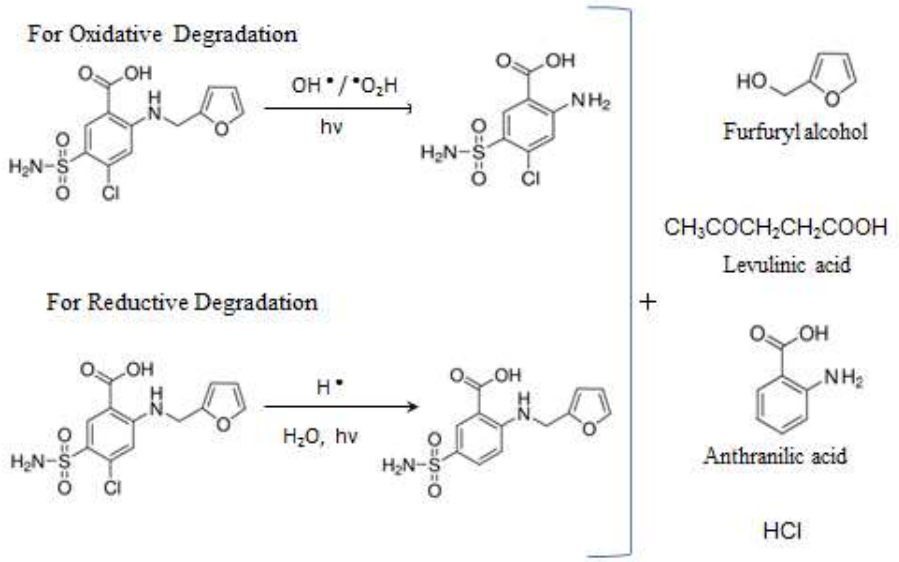

Plausible schematic routes for degradation of furosemide into fragments

Conclusions:

Nanoparticles of ZnO under doped and undoped conditions are employed as catalyst to bring about the oxidative and reductive degradations of furosemide. Irradiation sources

such as solar and UV are profusely used. Based on the rate coefficient values, the trend set observed is solar irradiations produced higher extent of degradation of furosemide drug Lasix than UV irradiations. In case of ZnO system, incorporation of dopants have altered both the morphology and as well as photocatalytic activity of nano ZnO particles. The increase in bandgap energy and decrease in crystal sizes show the dopant effects in ZnO wurtzite crystals. These observations go in hand that the catalyst involved with higher efficiency in the oxidation reaction exhibited lower efficiency in the reduction reaction conditions.

Acknowledgement:

The PXRD and GC-MS studies were supported by Dr.Sugirdha, Central-XRD and Professor Dr.G.Sekhar, Department of Chemistry, IIT Madras respectively.

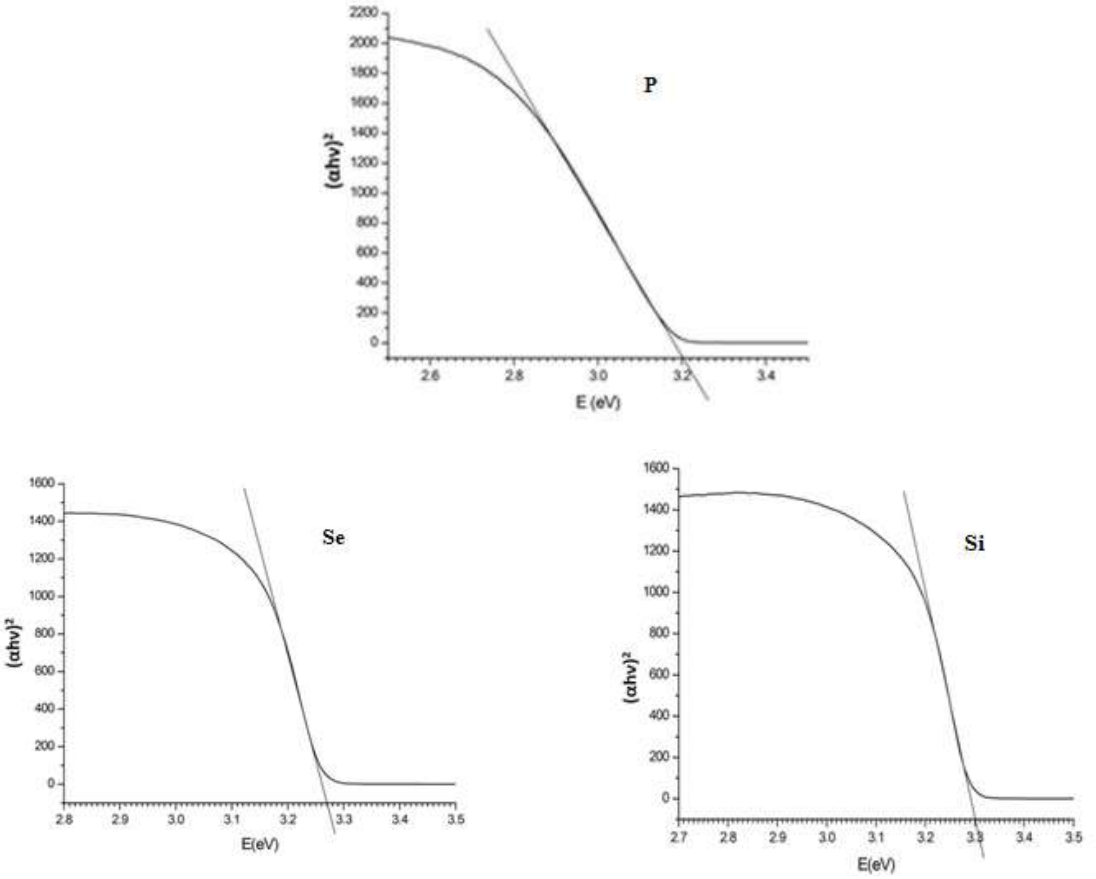

Fig 1: UVDRS plots of undoped ZnO (P), SeO_2 doped (Se) and SiO_2 doped ZnO nanoparticles (Si) respectively.

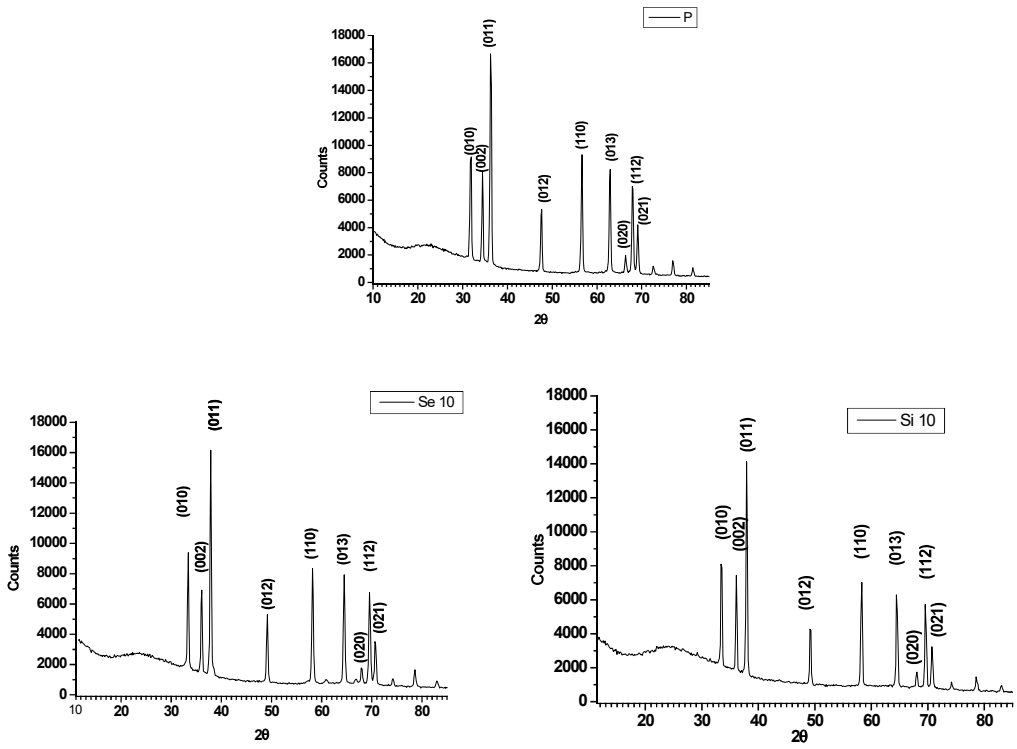

Figure 2: PXRD of undoped ZnO (P), SeO_2 doped (Se 10) and SiO_2 (Si 10) doped ZnO nano particles respectively

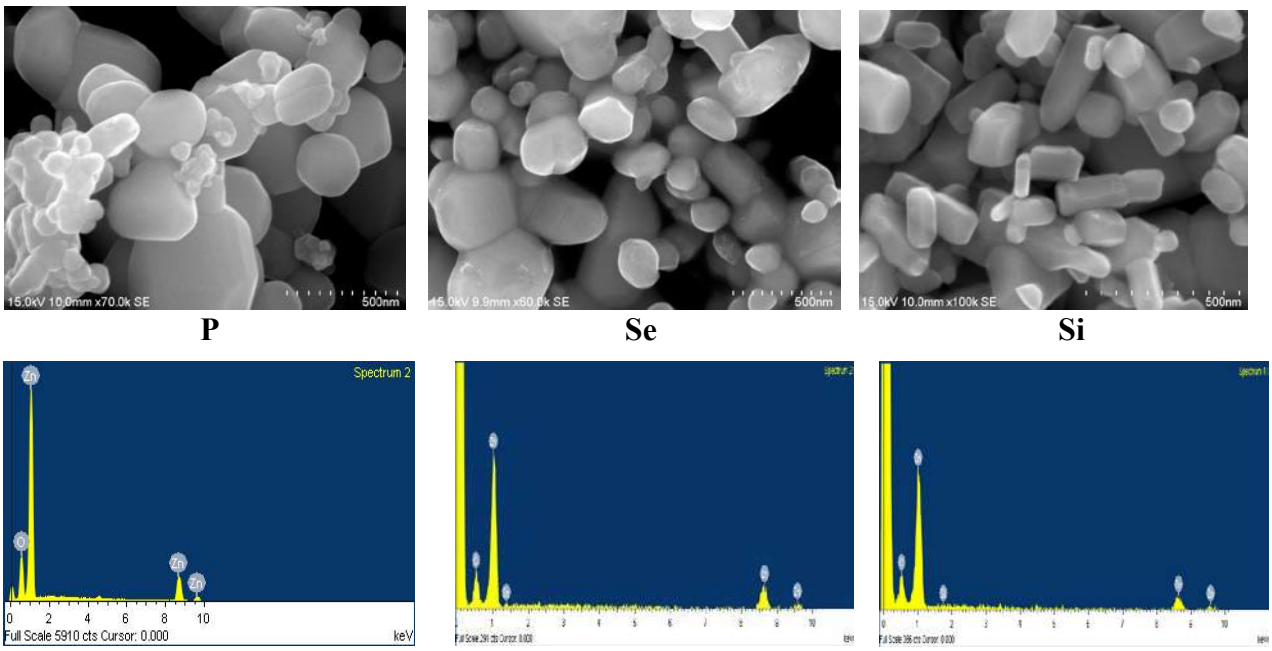

Figure 3: FESEM images and EDAX images of undoped ZnO (P), SeO_2 doped (Se) and SiO_2 (Si) doped ZnO nanoparticles respectively

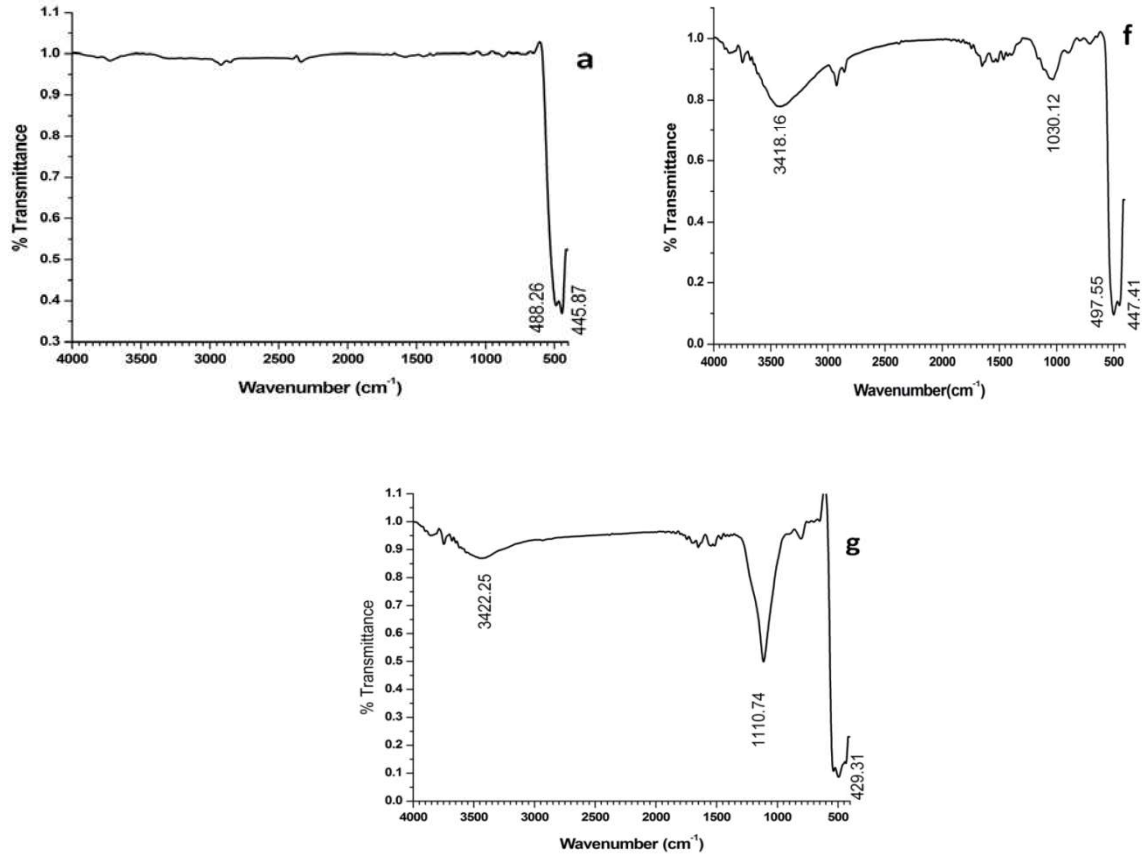

Figure 4: FTIR spectrum of undoped ZnO (a), SeO_2 (f) doped and SiO_2 (g) doped ZnO nanoparticles respectively.

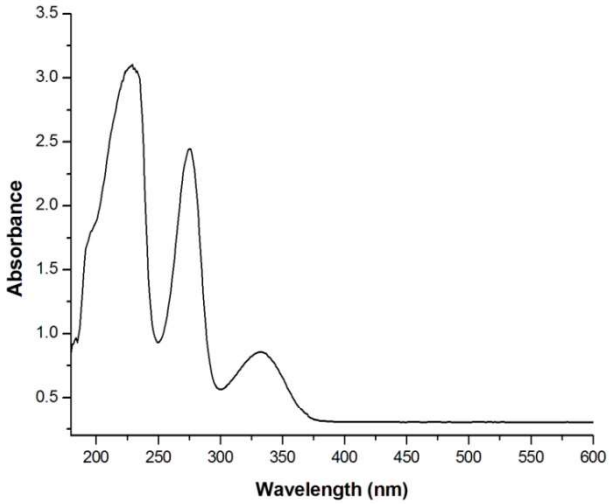

Fig 5: Typical UV-VIS spectrum of Lasix (Furosemide) drug

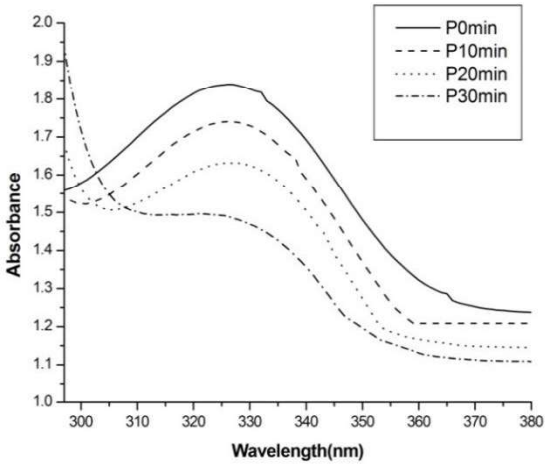

Fig 6: UV-VIS stacked spectra of Lasix degradation

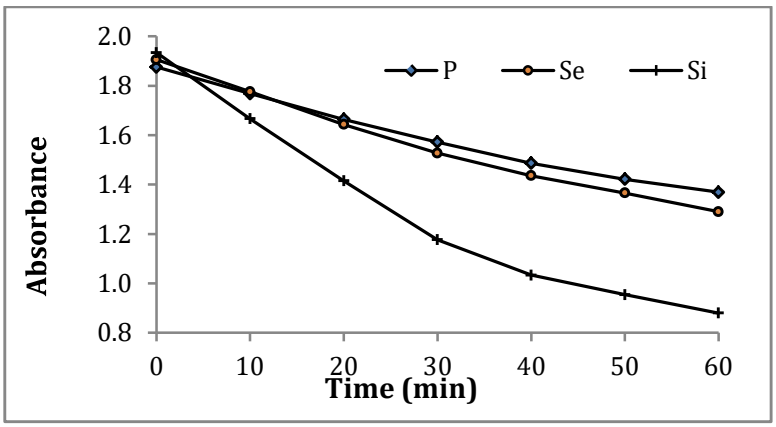

Fig 7: Absorbance versus time plot for solar assisted oxidative degradation of Lasix by catalysts P: ZnO; Se: SeO_2 and Si: SiO_2 doped ZnO respectively.

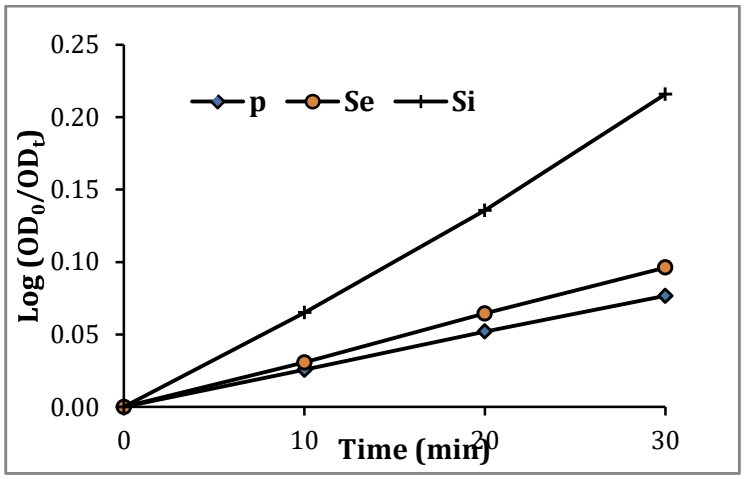

Fig 8: Pseudo first order kinetic plots for solar assisted oxidative degradation on Lasix by P: ZnO; Se: SeO_2 and Si: SiO_2 doped ZnO respectively

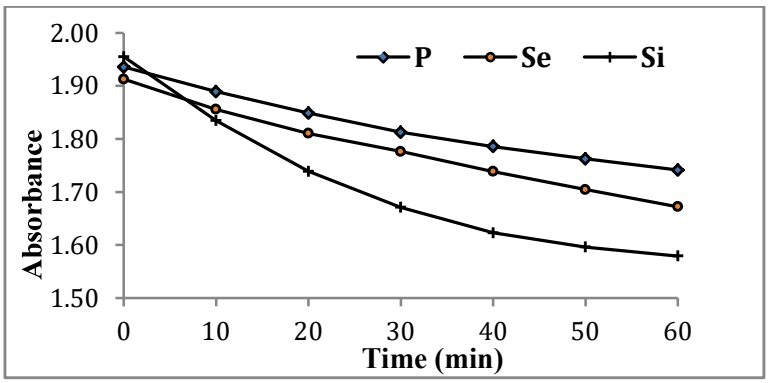

Fig 9: Absorbance versus time plot for UV assisted oxidative degradation by catalysts P: ZnO; Se: SeO_2 and Si: SiO_2 doped ZnO respectively.

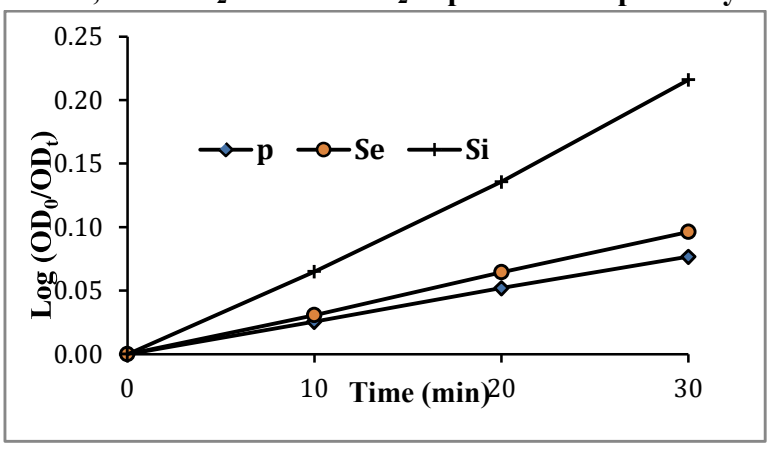

Fig 10: Pseudo first order kinetic plots for UV Assisted oxidative degradation by catalysts P: undoped ZnO; Se: SeO_2 and Si: SiO_2 doped ZnO respectively.

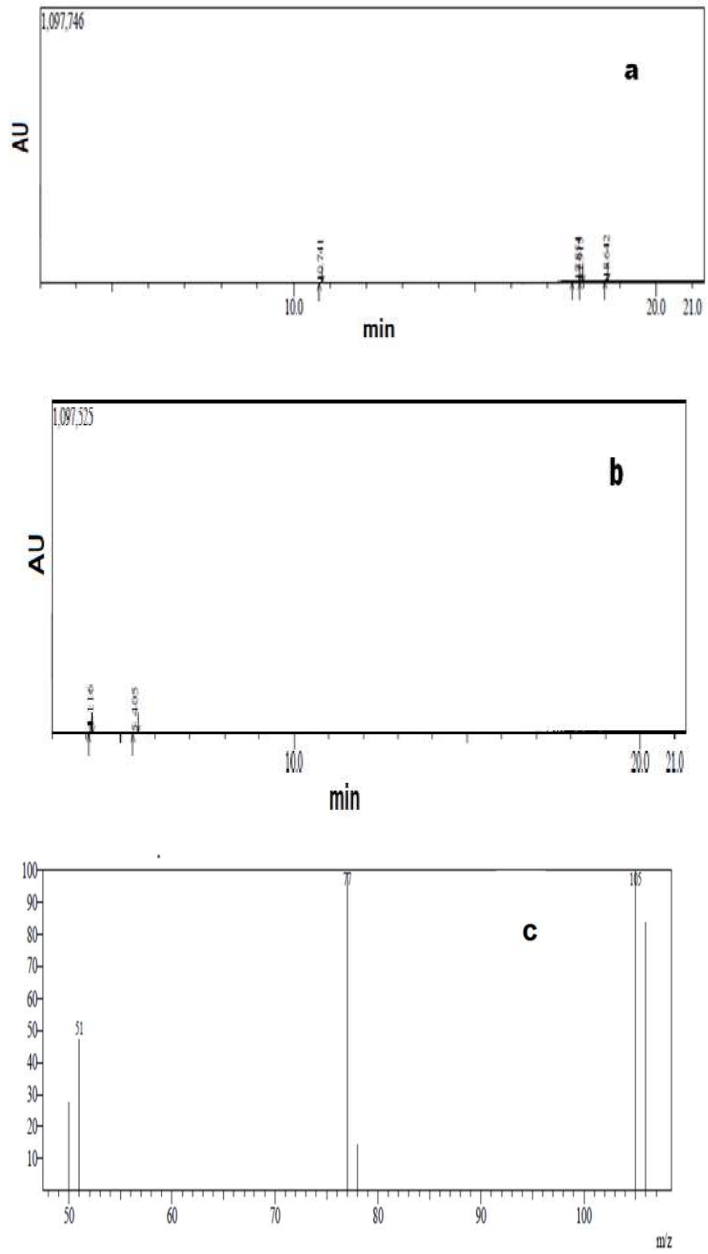

Fig 11: (a) GC pattern of Lasix (b) GC pattern of degraded Lasix (c) Mass spectra of degraded Lasix

Table 1: Band gap energy and Crystal size measurements for pure ZnO nanoparticles and doped ZnO nanoparticles.

Catalyst	Band gap energy values (eV)	Crystallite size from PXRD measurements (nm)
ZnO	3.20	30.0
SeO_2-ZnO	3.27	22.0
SiO_2-ZnO	3.3	17.0

Table 2: Comparison of Absorbance variation with time of Lasix (furosemide) under Oxidative degradation in solar irradiation

Catalyst	Time (min)	0	10	20	30	40	50	60
P	OD values	1.8754	1.7682	1.6639	1.572	1.4862	1.4215	1.3689
Se		1.9056	1.7756	1.6428	1.5269	1.4357	1.3659	1.2896
Si		1.934	1.6662	1.415	1.1764	1.0335	0.9541	0.8796

Table 3: Pseudo first order rate constant values ($x10^{-4}s^{-1}$) for photo catalytic oxidative degrsadation of Lasix by the nano catalysts

Irradiations	ZnO	SeO_2 dopant	SiO_2 dopant
Solar	1.97	2.48	5.51
UV	0.73	0.84	1.73

Table 4: Pseudo first order rate constant values ($x10^{-4}s^{-1}$) for solar assisted reductive degradation of Lasix catalysed by nanoparticles

Drug	ZnO	SeO_2 dopant	SiO_2 dopant
Lasix (Furosemide)	4.62	2.44	2.25

References:

1. K. Samal, S. Mahapatra, Md H.Ali, Energy Nexus, 6, 100076, 2022.
2. A.N. Pestryakov, ACS, *222*, U322-U322, 2022.
3. B. Bethi, CEP:PI, 109, 178, 2016.
4. D. Astruc, F. Lu and J. Ruiz Aranzaes, Angew.Chem.Int.Ed., 44, 7852, 2005.
5. N. S. Parmar and K. G. Lynn, Appl. Phys. Lett., 106. 022101,2015.
6. Y. Yu *J. Phys. Chem. C*, 118 (24), 12727, 2014.
7. A. Catellani and A. Calzolari, Materials, 10(4), 332, 2017.
8. A. R. Puigdollers, F. Illas, and G. Pacchioni, *J. Phys. Chem. C*, 20 (8), 4392, 2016.
9. M. Louhich, S. Romdhane, A. Fkiri, L. Smiri, H. Bouchriha, Applied Surface Science, 356, 998, 2015.
10. A. Majid, F. Javed, S. Akhtar, U. Saleem, F. Anwar, B. Ahmad, A. Nadhman, G. Shahnaz, I. Hussain, S.Z. Hussain and M.F. Sohail**,** J. Mater. Chem. B**,** 8**,** 8444, 2020.

11. A.S. Rini, Y. Rati, M. Agustin, Y. Hamzah and A. A. Umar, Sains Malaysiana 49(12), 3055, 2020.
12. A. Kuc, Chemical Modelling, RSC, 11, 1, 2014.
13. H. R. Pant, Ceram. Int. 38, 2943, 2012.
14. P. Coudray, Y. Moreau, P. Etienne and J. Porque, Proc. SPIE 10290, Sol-Gel and Polymer Photonic Devices: A Critical Review, 102900C, USA, 237, July, 1997.
15. C. Brunelli, C. Bicchi, A. D. Stilo, A. Salomone and M. Vincenti, J. Sep. Sci., 29, 2765, 2006.
16. M. Balouiri, M. Sadiki and S. K. Ibnsouda, J. Pharm. Anal., 6 (2), 71, 2016.
17. N.B. Saleh , D.J. Milliron, N. Aich, L.E. Katz, H.M. Liljestrand and M. J.Kirisits, Science of the Total Environment, 568, 926, 2016.
18. C.Mao, L.Fang, H. Zhang, W. Li, F. Wu, G. Qin, H. Ruan and C. Kong, J. Alloys Compd., 676, 135, 2016.
19. S.Talukdar and R. K. Dutta, RSC Adv., 6, 928, 2016.
20. S. Kumar, P. Chauhan and V. Kundu, J. Mater. Sci.: Mater. Electron, 27(3), 3103, 2016.
21. L. Wang, S. Zheng and H. Chen, J. Electron. Mater., 46, 5, 2017.
22. M.Samadi, M. Zirak, A Naseri, E. Khorashadizade and A. Z. Moshfegh, Thin Solid Films, 605, 2, 2016.
23. T. Ruf, S. Repp, J. Urban, R. Thomann and E. Erdem, Journal of Nanoparticle Research 18, 1, 2016.
24. K.S. Babu, A.R. Reddy, C. Sujatha, K.V. Reddy and A.N. Mallika, J. Adv. Ceram., 2 (3), 260, 2013.
25. A.Vanaja, G. V. Ramaraju and K. Srinivasa Rao, Indian J Sci Technol., 9 (12), 1, 2016.
26. S. Ananda, Am. Chem. Sci. J., 4 (5), 616, 2014.
27. I. Khan, S. Khan, R. Nongjai, H. Ahmed and W. Khan, Optical Materials, 35 (6), 1189, 2013.
28. I .L.T. Dias, J. L.S. Martins and G.O. Neto, Anal. Lett., 38,1159, 2005.
29. S Katsura, N. Yamada, A. Nakashima, S. Shiraishi, T. Furuishi and H. Ueda, Chem. Pharm. Bull. 63, 617, 2015.
30. S.C. Broch, J.E. Romero and M.C.G.A. Coque, J. Pharm. Biomed. Anal., 23, 803, 2000.
31. X. Pang, C. Chen, H. Ji, Y. Che and W. Ma, Molecules, 19, 16291, 2014.